

Article

Modified Droop Control for Microgrid Power-Sharing Stability Improvement

Ahmed Rashwan¹, Alexey Mikhaylov², Tomonobu Senjyu³ , Mahdihyeh Eslami⁴ , Ashraf M. Hemeida^{1,*} 
and Dina S. M. Osheba⁵

¹ Department of Electrical Engineering, Faculty of Energy Engineering, Aswan University, Aswan 81528, Egypt; engrashwan@aswu.edu.eg

² Department of Financial Markets and Financial Engineering, Financial University under the Government of the Russian Federation, 125167 Moscow, Russia; alexeyfa@fa.ru

³ Department of Electrical and Electronics Engineering, Faculty of Engineering, University of the Ryukyus, Nishihara 903-0213, Japan; b985542@tec.u-ryukyu.ac.jp

⁴ Department of Electrical Engineering, Kerman Branch, Islamic Azad University, Kerman 7635168111, Iran; m.eslami@iauk.ac.ir

⁵ Department of Electrical Engineering, Faculty of Engineering, Menoufia University, Shebin El Kom 32511, Egypt; dina.asheba@sh-eng.menofia.edu.eg

* Correspondence: ashraf@aswu.edu.eg

Abstract: Isolated microgrid (IMG) power systems face the significant challenge of achieving fast power sharing and stable performance. This paper presents an innovative solution to this challenge through the introduction of a new droop control technique. The conventional droop controller technique used in inverter-based IMG systems is unable to provide satisfactory performance easily, as selecting a high droop controller gain to achieve fast power sharing can reduce the system's stability. This paper addresses this dilemma by proposing a modified droop control for inverter-based IMGs that effectively dampens low-frequency oscillations, even at higher droop gain values that would typically lead to instability. The design is described step-by-step, and the proposed controller's effectiveness is validated through time domain simulation analysis. The results demonstrate the significant improvement in stability and fast power sharing achieved with the proposed controller. This innovative technique presents a promising solution for achieving fast power sharing and stable performance in IMG power systems.

Keywords: microgrid; droop control; power sharing; renewable energies



Citation: Rashwan, A.; Mikhaylov, A.; Senjyu, T.; Eslami, M.; Hemeida, A.M.; Osheba, D.S.M. Modified Droop Control for Microgrid Power-Sharing Stability Improvement. *Sustainability* **2023**, *15*, 11220. <https://doi.org/10.3390/su151411220>

Academic Editors: Chun-Lien Su, Te-Tien Ku and Chia-Hung Lin

Received: 13 June 2023
Revised: 10 July 2023
Accepted: 14 July 2023
Published: 19 July 2023



Copyright: © 2023 by the authors. Licensee MDPI, Basel, Switzerland. This article is an open access article distributed under the terms and conditions of the Creative Commons Attribution (CC BY) license (<https://creativecommons.org/licenses/by/4.0/>).

1. Introduction

Microgrids are quickly emerging as a key tool for reducing our dependence on fossil fuels while improving the efficiency and reliability of our power grids. By using localized power generation and distribution, microgrids are able to offer greater independence from central power grids, reducing the risk of blackouts and other disruptions [1]. Additionally, the development and implementation of microgrids require expertise from a wide range of scientific disciplines, including electrical engineering, power electronics, and computer science, to ensure that they operate efficiently and effectively. As we continue to explore new approaches to energy generation and distribution, microgrids will undoubtedly play a crucial role in our transition toward a more sustainable and resilient energy system that is better equipped to meet the needs of society, while also helping to mitigate the harmful impacts of climate change [2].

A microgrid (MG) is a small-scale power system that comprises renewable and nonrenewable distributed generation (DG), power electronic devices, energy storage systems, and different loads. An MG may be a grid-connected or isolated power system. Due to nonlinear power electronic devices and DG power sources, it has several concerns with

power quality [3,4]. In order to have a smooth connection between DGs and MGs, DC/DC converters and DC/AC inverters have a major role in power flow management [5]. The droop controller has been widely used to achieve power sharing in both direct current (DC) and alternating current AC MGs. Also, it has been used to coordinate between two AC and DC MGs [6].

The droop controller comprises series-connected different linear control loops which are the current control loop, voltage control loop, and filter control loop [7,8]. It simulates the power-sharing characteristics of a synchronous generator based on the frequency of output voltage correlated to real power, reactive power, and magnitude of output voltage [9,10]. The droop control approach is an interesting technique for regulating the load-sharing between two inverters or more in an isolated microgrid (IMG). It organizes the fundamental frequency management without a communication link. The absence of a communication link between inverters simplifies the controller's design, decreases the system's complexity, and reduces the board's graphical area [11–15]. The primary role of the inverter controller is to regulate both system voltage and frequency as well as to share active and reactive power in an IMG. A popular solution is to employ a frequency droop controller, which allows the parallel converters to be regulated locally to supply the system with the necessary active and reactive power by controlling the magnitude and frequency which are two independent quantities [16]. The droop controller uses the measured values of output currents and voltages at an inverter's terminal to calculate the inverter's active and reactive power. Two cascaded inner-loop voltage and current controllers are regulated to maintain the voltage and frequency steady while servicing loads in an MG [17].

Since the system has no inertial portion, the transient characteristics of the inverter connected to the MG are crucial. Therefore, the controller design is critical in the IMG on which the system's stability depends [18]. The authors in Refs. [19–23] propose a comprehensive small signal model design for a droop-controlled inverter connected to an IMG. The authors determined that the system's low-frequency modes are mostly responsive to the droop controller's settings. Consequently, even slight changes in the controller parameters will influence the overall MG's stability. Reference [24] presents an energy supervision system in the IMG considering stability limits because of droop control. Then, several studies were performed to provide the small signal model in the presence of load dynamics. Reference [25] investigates the transient stability behavior of a power system integrated with several distributed generators through power electronic converters. In [26], structured singular values are used to examine the effectiveness of voltage and current controllers in enhancing the stability of a stand-alone distributed generation (DG) unit. Consequently, a current controller based on discrete-time sliding mode has been produced. Load-sharing control of several DG systems has been studied based on new droop and average power approach for isolated power systems [27–29]. The preceding studies concluded that the stability of the IMG primarily depends on the controller. A fast sharing for the load changes is necessary to prevent the inverter from being overloaded to avoid voltage collapse at the inverter terminal.

Many studies have proposed various controllers for improving dynamic performance. Paper [30] improves transient responsiveness by including a derivative-integral term in a traditional droop controller. Paper [31] proposes a three-stage auxiliary controller based on a power system stabilizer (PSS). In [32], an adaptive derivative droop control is developed that enhances the MG's dynamic performance without affecting its steady-state response. Reference [33] proposes a feed-forward adjustment to improve the resilience of MG stability to droop factors. Reference [34] proposes a PSS-based damping controller for a hybrid inverter and synchronous machine-based distributed generator MG's. Although previous solutions improved MG stability, most techniques are challenging to implement due to the numerous tuning parameters required. Furthermore, many controllers eliminate the decoupling between real and reactive power, affecting the system's analysis and performance.

Achieving adequate load-sharing requires substantial angle droop gains, especially for a weak grid. However, the system's overall stability is negatively influenced by high droop

gains, as demonstrated by eigenvalue analysis and simulations. PSS-based controllers are developed to stabilize the primary droop control loop. PSS-based controllers can provide further dampening to low-frequency oscillations. Compared with earlier efforts, the proposed technique only modifies the power controller in order to provide the necessary dampening. The technique described here can be designed and applied in any inverter MG setup (radial/mesh). Decoupling between active and reactive loops is essential for easier analysis. The new proposed techniques also do not need optimization algorithms compared to the traditional PSS, which leads to unsatisfactory performance. Furthermore, optimizing several parameters might be time-consuming. The optimization techniques primarily depend on calculating the exact phase lag delay caused by the output filter. Moreover, compared to the droop controller technique in [29–34], the proposed controller is a single stage, reducing the number of parameters to calculate and streamline the controller's design process.

In this paper, a novel lead compensator is introduced, specifically designed for use with the conventional droop controller utilized in inverter-based autonomous microgrids. The proposed controller addresses the trade-off between quicker power sharing and system stability at higher droop coefficients, a significant breakthrough in this field. A step-by-step approach for developing the auxiliary controller is presented, with careful selection of two key parameters (T_1 , T_2) to achieve optimal performance. By incorporating an auxiliary signal that compensates for the filter delay, the low-frequency modes can be effectively dampened out. The proposed controller enhances the microgrid's stability limit while ensuring rapid power sharing at both lower and higher droop coefficients. This guarantees that large steady-state frequency deviations and frequency/power oscillations are prevented without sacrificing power sharing. Simulation results are presented under various operating conditions to validate the controller's effectiveness, and an eigenvalue analysis of the modified system is provided to demonstrate how the critical low-frequency mode shifts from the right to the left half of the s-plane.

The primary contributions of this study are highlighted below:

- Development of a modified droop controller-based inverter for isolated microgrid (IMG) systems.
- Calculation of the new control parameters without the use of optimization techniques, making the proposed approach a generic strategy that is easy to implement in any system while maintaining active and reactive power decoupling.
- Achievement of fast power sharing for load changes even at lower droop coefficient levels.

These contributions represent significant advancements in the design of IMG power systems, offering a simple yet effective solution for improving stability and power-sharing capabilities.

This paper is organized as follows. Section 1 provides the introduction and literature review. Section 2 presents the conventional droop control technique. The design of the proposed PSS is discussed in Section 3, followed by the presentation of simulation results in Section 4. Finally, this paper concludes in Section 5.

2. Conventional Droop Control for Power Sharing

The proposed strategy is introduced by a single-line diagram as introduced in Figure 1. It comprises three inverters with four loads. The inverters are assumed to have a constant direct current (DC) source. In the IMG, the inverters maintain the frequency, voltages, and load demand. All three inverters are assumed to provide the MG's entire power demand. The system can easily extend to additional inverters and loads. The inverter power controller regulates the active power based on the frequency and the reactive power based on the output voltage. To investigate the performance of the proposed controller for quicker power sharing and stability, the active power and frequency relationship has been monitored. The inverter system's control methodology has three cascaded control levels (voltage, current, and droop (Figure 2)) and is discussed in detail in the following sections.

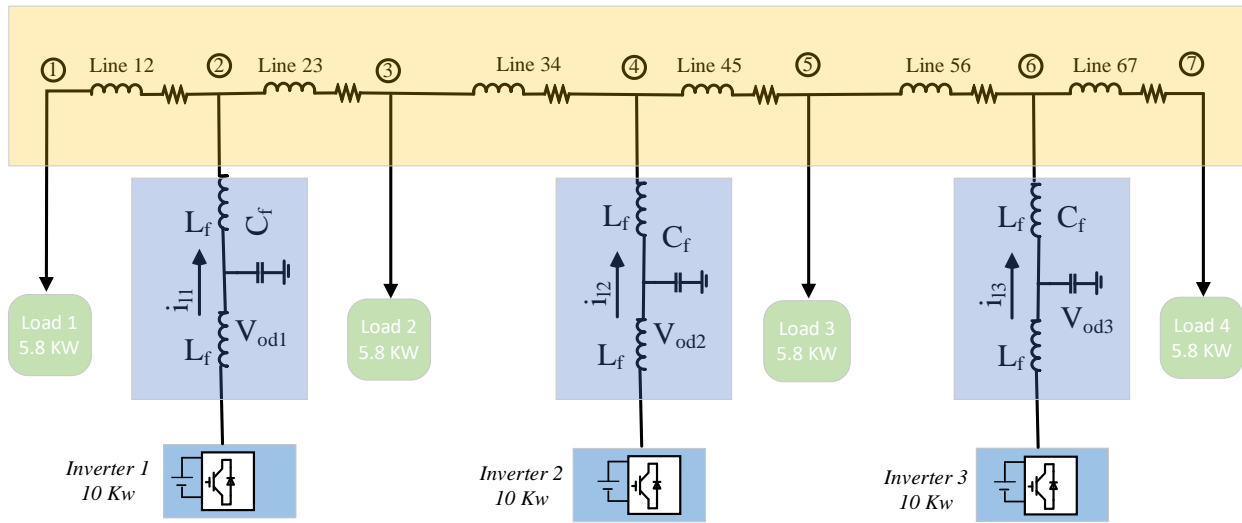


Figure 1. The single-line diagram of the test system [15].

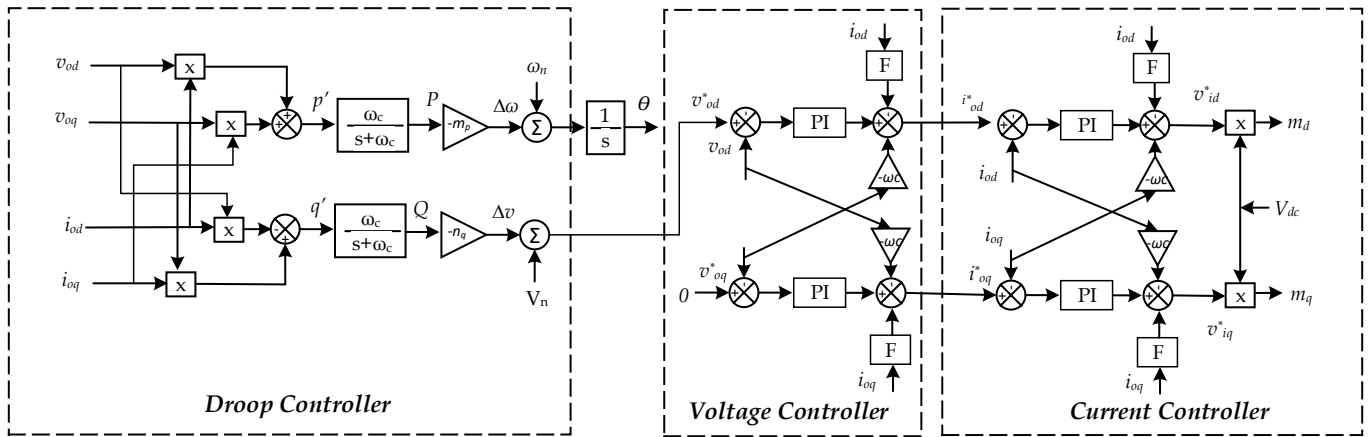


Figure 2. Cascaded control technique for the inverter [5].

2.1. Droop Controller

The primary droop control is the first stage of the inverter control strategy. The droop controller regulates both voltage and frequency based on the present loading circumstances. It primarily depends on calculating the real and reactive power and inserts a droop coefficient to produce frequency and voltage Figure 2. The instantaneous power produced at the output terminals of the inverter could be expressed by Equation (1).

$$\tilde{P} = v_{od}i_{od} + v_{oq}i_{oq} \tag{1}$$

$$\tilde{q} = -v_{od}i_{oq} + v_{oq}i_{od} \tag{2}$$

where v_{od}, i_{od} is the d -axis voltage and current and v_{oq}, i_{oq} is the q -axis voltage and current. A low-pass filter operating at a cutoff frequency ω_c is used to obtain the fundamental components P and Q from instantaneous powers as follows:

$$P = \frac{\omega_c}{S + \omega_c} \tilde{P} \tag{3}$$

$$Q = \frac{\omega_c}{S + \omega_c} \tilde{q} \tag{4}$$

The new operating frequency and output voltage can be estimated based on the droop gain relations in Figure 2. An intelligent droop coefficient m_p represents the f - P drooping behavior, whereas the droop coefficient n_q represents the V - Q droop behavior. Therefore, the new frequency and voltage values are calculated as follows:

$$\omega = \omega_n - m_p P \quad (5)$$

$$v_{od}^* = V_n - n_q Q, v_{oq}^* = 0 \quad (6)$$

where ω_n is the operating frequency, V_n is the operating voltage, ω is the new operating frequency, v_{od}^* is the d -axis reference voltage, and v_{oq}^* is the q -axis reference voltage. The coefficients m_p and n_q , also known as droop coefficients, can be calculated using the following relationships:

$$m_p = \frac{\omega_{max} - \omega_{min}}{P_{max}} \quad (7)$$

$$n_q = \frac{V_{max} - V_{min}}{Q_{max}} \quad (8)$$

where m_p and n_q are chosen in the autonomous mode, such that the load change is shared among the parallel inverters in operation based on their rating.

2.2. Voltage and Current Controller

Figure 2 illustrates that the voltage control loop is responsible for the bus voltage stability, whereas the current loop protects the insulated-gate bipolar transistors against over-currents. A proportional–integral controller (PI) was devolved to generate the reference current voltage. The PI controller is standard, with decoupled and feedforward control loops. The voltage controllers' dynamics can be given by

$$i_d^* = K_{pv}(v_{od}^* - v_{od}) + K_{iv} \int (v_{od}^* - v_{od}) dt - \omega^* C_f v_{oq} + F i_{od} \quad (9)$$

$$i_q^* = K_{pv}(v_{oq}^* - v_{oq}) + K_{iv} \int (v_{oq}^* - v_{oq}) dt - \omega^* C_f v_{od} + F i_{oq}, \quad (10)$$

where K_{pv} is the proportional gain; K_{iv} is the integral gain; C_f is the filter capacitance; and the feed forward gain is represented by F .

Similarly, the voltage across the filter inductor is obtained using a standard PI current controller. The dynamics are given by

$$v_d^* = K_{pi}(i_d^* - i_d) + K_{ii} \int (i_d^* - i_d) dt - \omega^* L_f i_q + v_{od} \quad (11)$$

$$v_q^* = K_{pi}(i_q^* - i_q) + K_{ii} \int (i_q^* - i_q) dt - \omega^* L_f i_d + v_{oq}, \quad (12)$$

where proportional and integral gains are represented by K_{pi} and K_{ii} , respectively.

A small signal dynamic model was developed to study the dynamic behavior of MG power sharing. The equivalent differential equations model has been linearized to accurately simulate the MG dynamics of the network and load. This could be represented by Equation (13).

$$\Delta \dot{x} = A \Delta x + B \Delta u. \quad (13)$$

The state vector in Equation (13) will represent the studied system in Figure 1, containing three inverters and their loads.

Figure 3 shows the MG system's eigenvalues, showing that the MG system can be classified into three primary bandwidths. The power-sharing controllers dictate a low bandwidth (2–10 Hz), whereas the voltage control loop dictates a medium bandwidth

(400–600 Hz). The current controller and the LC filters produce a high-frequency bandwidth (more than 1.5 kHz). The current control loop's maximum bandwidth depends on the inverter's switching frequency. The switching frequency is designed according to the rating of the inverter and switching losses. However, the resonance frequency should be carefully designed to avoid the LC filter's harmonic resonance and low-order harmonics. Therefore, considering these constraint issues, the design of current controller inverter for medium and high bandwidth could be within 1–1.5 kHz. Since MG inverters must supply regulated power, the reference current vector is created frequently for the inner current loop using a voltage control loop. Figure 3 shows that the MG system's primary dynamics are derived by the power-sharing states.

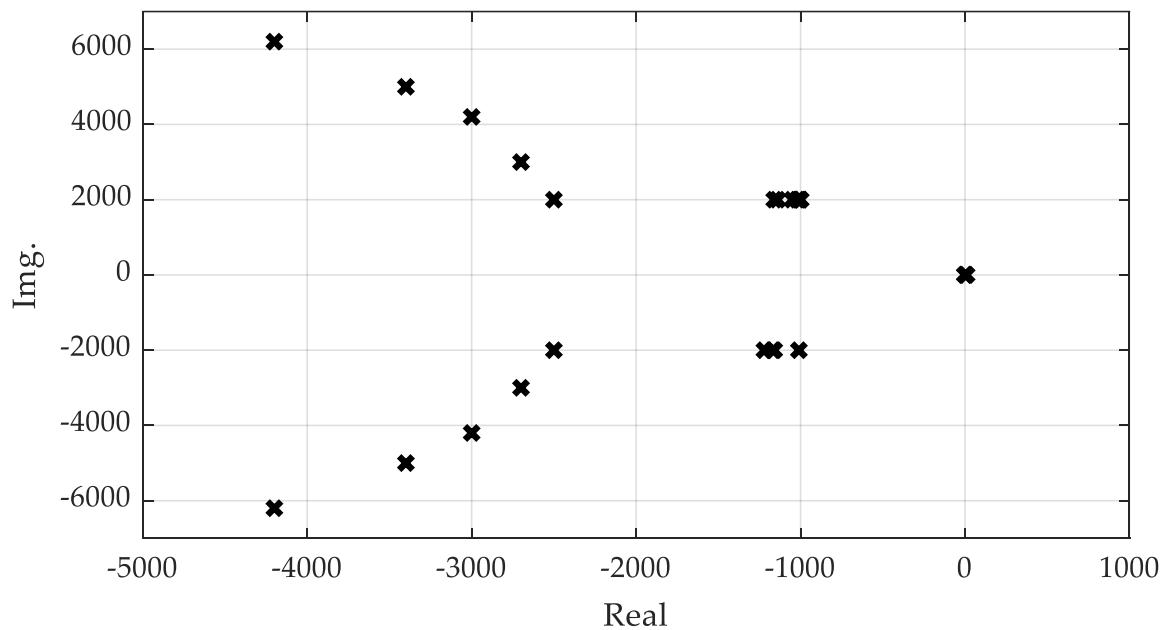


Figure 3. The eigenvalues of the microgrid studied system.

Figure 4 displays a trace of the dominating low-frequency mode that could be evaluated using eigen-participation analysis. Figure 4 shows that the operating environment greatly affects the damping behavior of the low-frequency mode. Figure 4 shows that increasing the inverter unit's output power can make the operation unstable. Even modest changes near the operating point significantly affect the relative stability, resulting in power oscillations. Regarding the droop coefficient value, the MG power-sharing operation and concept deepen the angular frequency difference between the inverter's outputs. The power sharing between sources varies until the new frequency value is defined in Equation (3).

Figure 5 describes the relationship between power changes versus frequency droop changes, where power P versus the frequency f is linear. Equation (5) shows that as the term $m_p P$ increases, the frequency drop becomes sufficient so that the nearest inverter will increase its power to share the load. However, the change in frequency is delayed due to the filter lag time delay causing oscillations in the frequency, which can be overcome by increasing the coefficient (m_p), forcing the inverter to push the power instantly. However, increasing the coefficient m_p should be performed carefully because it affects the system's stability. Therefore, a tradeoff occurs between the fast power sharing and the system's stability in the conventional technique.

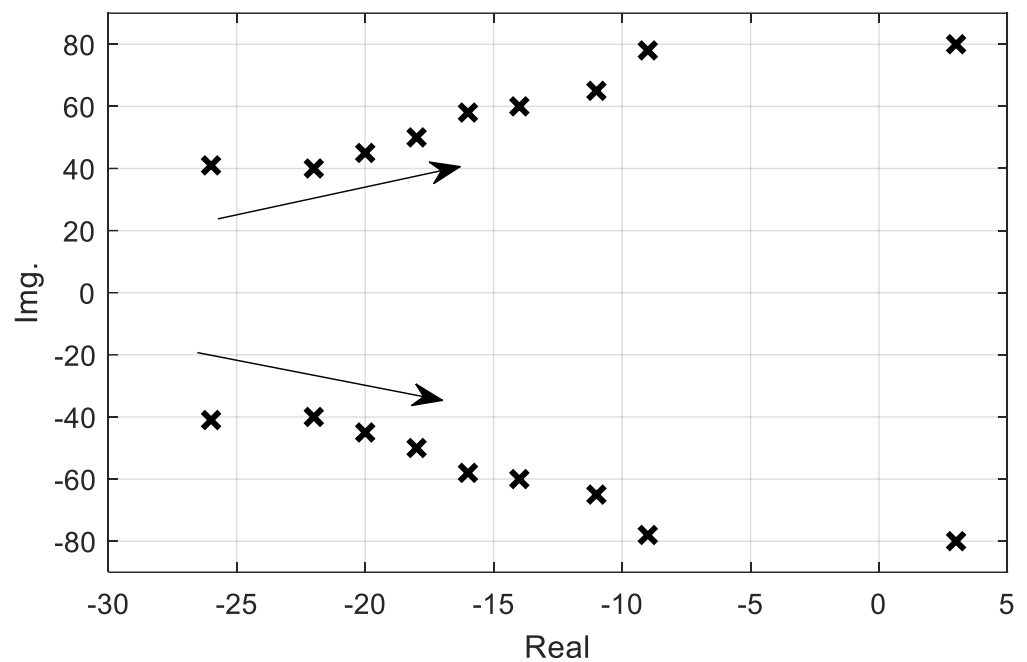


Figure 4. A trace of the dominating low-frequency mode.

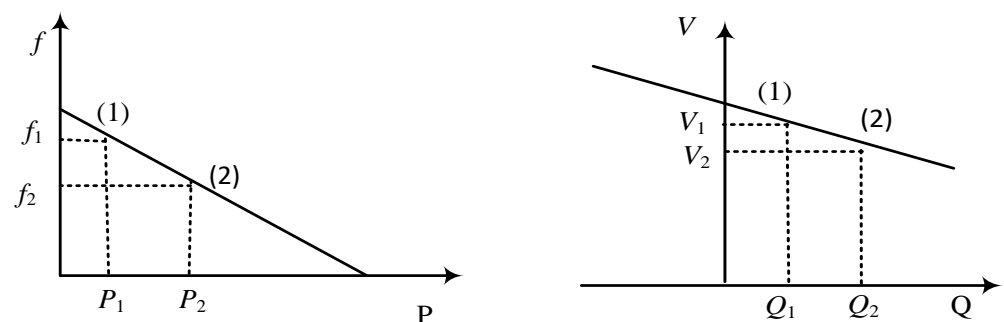


Figure 5. Power versus frequency droop and voltage versus reactive power droop [21].

In a parallel multi-inverter system with droop control, maintaining a stable voltage level at the PCC is crucial for ensuring a reliable power supply. The droop control method adjusts the inverter output voltage based on the Q/V curve characteristics and the reactive power output based on the deviation of the output voltage from the reference voltage. When the inverter output voltage is higher than the PCC voltage, the droop control causes the inverter to decrease its output voltage and supply less reactive power to the system. Conversely, when the inverter output voltage is lower than the PCC voltage, the droop control causes the inverter to increase its output voltage and supply more reactive power to the system, which raises the voltage level at the PCC. To achieve optimal performance in the system, the droop parameters, such as the droop gain and voltage reference, can be adjusted by the system operator. By doing so, the reactive power output of the inverters can be controlled and the voltage level at the PCC can be regulated, even in situations where there are fluctuations in load demand.

3. The Proposed Droop Control for the Microgrid System

The response to load changes in the IMG is delayed due to the lag of the low-frequency filter; therefore, a lead compensator should be included to compensate for this delay. The concept of the compensator is standard in the synchronous-based system, but here it is applied to the inverter-based system. Figure 6 illustrates a block diagram for the proposed controller, comprising a gain block and an integral lead compensator transfer function. The original frequency deviation is increased by the signal output of the controller

to compensate for the delay time from the low-pass filter. The design procedure of the compensator depends on the delay angle deviation at a higher (m_p). Therefore, if the low-pass filter causes a delay by angle (θ), the lead compensator will be calculated as follows:

$$-\theta + \angle \frac{sT_1 + 1}{sT_2 + 1} = 0. \tag{14}$$

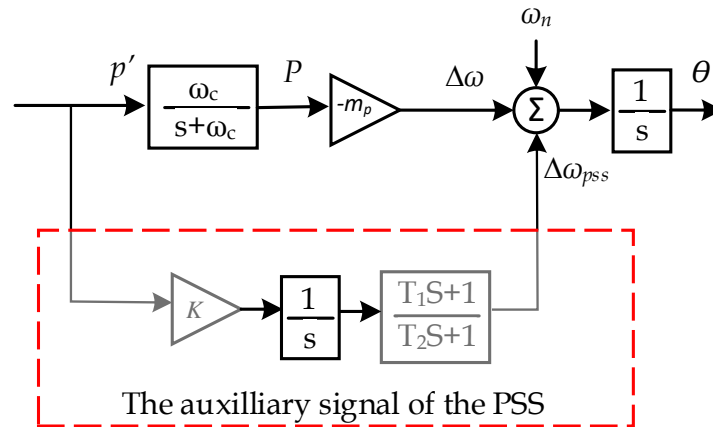


Figure 6. The proposed modified droop control signal.

Therefore, for a defined (θ), one of the time constants (T_1, T_2) is arbitrarily chosen and the other calculated. The gain K of the controller in Figure 6 is designed so that the magnitude of the frequency drop $\Delta\omega = -m_p P$ equals the compensator drop ($\Delta\omega_{pss}$).

Small signal analysis can effectively analyze dynamic performance and design control systems. The MG system’s state–space model is derived to study the proposed controller technique’s dynamic performance. Figure 7 illustrates a block diagram of the individual blocks of the system including an inverter, filter, droop control, current control, and voltage control. The mathematical procedures of obtaining the state–space model are abbreviated to obtain the relevant equations. The system equations (Equations (1)–(12)) can be linearized, yielding the following state–space model which presents a single inverter unit,

$$\frac{d}{dt} \begin{bmatrix} \Delta\delta \\ \Delta P \\ \Delta Q \end{bmatrix} = A_p \begin{bmatrix} \Delta\delta \\ \Delta P \\ \Delta Q \end{bmatrix} + B_{p\omega_{ref}} \begin{bmatrix} \Delta\omega_{ref} \end{bmatrix} + B_p \Delta f_{iv} \tag{15}$$

where

$$\Delta f_{iv} = \begin{bmatrix} \Delta i_{ld} & \Delta i_{lq} & \Delta v_{od} & \Delta v_{oq} & \Delta i_{od} & \Delta i_{oq} \end{bmatrix}^T. \tag{16}$$

Equations (15) and (16) present the linearized state–space model for the inverter unit. The model has three states: $\Delta\delta$, ΔP , and ΔQ , which represent the deviations in the phase angle, active power, and reactive power, respectively. The matrix A_p and vector B_p represent the coefficients of the linearized equations. The input to the system is the reference frequency ω_{ref} , and the disturbance is represented by the vector Δf_{iv} , which consists of deviations in the inverter unit’s voltage and current variables.

One more state will be added to the conventional state–space model (i.e., $\Delta\omega_{pss}$),

$$\Delta\omega_{pss} = \tilde{P} * K * \left(\frac{sT_1 + 1}{sT_2 + 1} \right). \tag{17}$$

Equation (17) adds a new state to the state–space model, which is $\Delta\omega_{pss}$, representing the deviation in the power system stabilizer (PSS) output. The equation describes the dynamics of the PSS output as a function of an input f_{ini} and a set of parameters K , T_1 , and T_2 . The PSS output is used to control the inverter unit’s output frequency.

The state–space Equation (15) is then linearized around its operating point,

$$\Delta\dot{\omega}_{pss} = \left(\frac{-1}{T_2}\right)\Delta\omega_{pss} + \left(\frac{K}{T_2}\right)f_{ini}\Delta f_{if} + \left(\frac{KT_1}{T_2}\right)f_{ini} * \frac{d}{dt}\Delta f_{if} \tag{18}$$

Equation (18) linearizes Equation (15) around its operating point to obtain the dynamics of the new state $\Delta\omega_{pss}$. The equation shows that $\Delta\omega_{pss}$ is a function of the input f_{ini} and the time derivative of the input $d/dt\Delta f_{if}$.

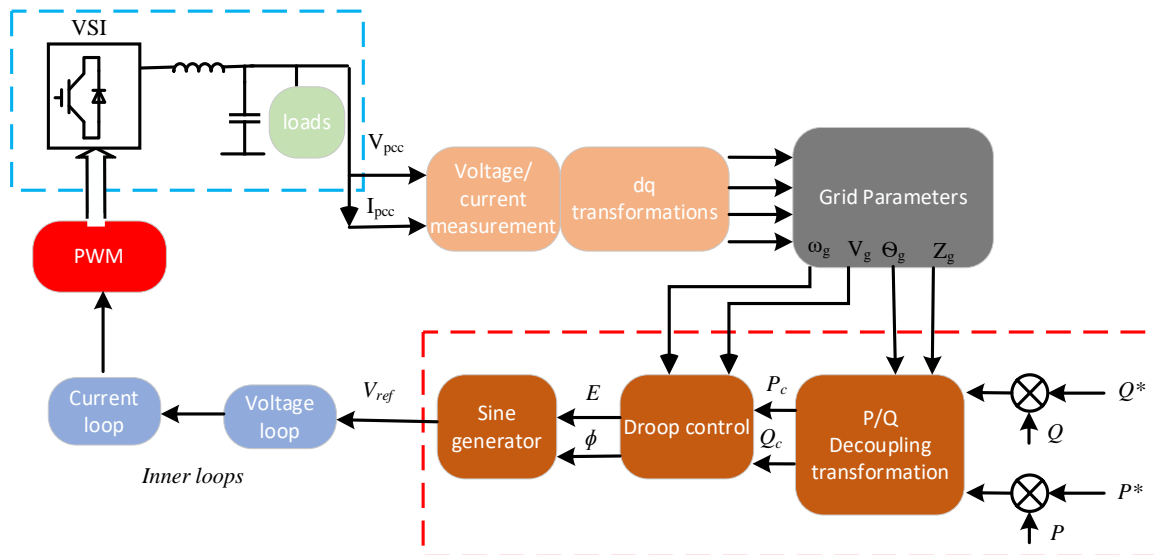


Figure 7. Control structure of the microgrid system [8].

Therefore, the first state $\Delta\delta$ in Equation (18) will be modified according to the new controller state as;

$$\Delta\omega = -m_p P - \Delta\omega_{pss} \text{ and} \tag{19}$$

$$\Delta\dot{\delta} = -m_p P - \Delta\omega_{pss} - \Delta\omega_{ref} \tag{20}$$

Equations (19) and (20) modify the first state $\Delta\delta$ in Equation (18) according to the new controller state, which is $\Delta\omega$. Equation (19) shows that $\Delta\omega$ is a function of the product of the controller gain m_p and the input power P , and the deviation in the PSS output $\Delta\omega_{pss}$. Equation (20) shows that the time derivative of $\Delta\delta$ is a function of $\Delta\omega$, $\Delta\omega_{ref}$, the product of the controller gain m_p , and the input power P .

The modified system’s state–space will be formed by integrating the conventional model’s state–space with the proposed controller model,

$$\Delta\dot{x}_p = A_p\Delta x_p + B_{pre}f\Delta\omega_{ref} + B_{p1}\Delta f_{iv} + B_{p2} * \frac{d}{dt}\Delta f_{iv}, \tag{21}$$

where $\Delta x_p = [\Delta\delta \ \Delta P \ \Delta Q \ \Delta\omega_{pss}]^T$.

Equation (21) presents the modified system’s state–space model, which integrates the conventional state–space model with the proposed controller model. The state vector Δx_p represents the deviations in the phase angle, active power, reactive power, and power system stabilizer output, respectively. The matrices A_p , B_{pre} , B_{p1} , and B_{p2} represent the coefficients of the linearized equations, where B_{pre} and B_{p1} are functions of the input $\Delta\omega_{ref}$ and the disturbance Δf_{iv} , respectively, and B_{p2} is a function of the time derivative of the disturbance $d/dt\Delta f_{iv}$. The state–space model can be used to design a control system that stabilizes the inverter unit’s output voltage and frequency.

Due to space limits, the numerous coefficients used in the preceding equations are not provided in this study. The complete MG's small signal model is created once the revised equations and necessary coefficients are established.

In the context of power systems, eigenvalues are used to analyze the stability of the system. Eigenvalues are the solutions to the characteristic equation of the system, which is obtained by linearizing the system equations around an operating point. The eigenvalues determine the behavior of the system in response to disturbances and are used to assess the system's stability. In the case of an inverter-based microgrid, the eigenvalues can be used to assess the stability of the system under different control schemes, such as conventional and modified droop controls that are proposed in this paper.

The results show that the system without any controller has two low-frequency modes, or oscillations, with eigenvalues of $0.00154 \pm 165.56 i$ and $-12.43 \pm 122.832 i$. These eigenvalues are in the right half of the complex plane, which indicates that the modes are poorly damped and unstable. However, when the modified droop control is applied, the eigenvalues of the system shift to the left half of the complex plane. The system now exhibits two new low-frequency modes with eigenvalues of $-14.87 \pm 96.98 i$ and $-17.987 \pm 187.965 i$. These eigenvalues are in the left half of the complex plane, which indicates that the modes are well-damped and stable. The shift in the eigenvalues to the left half of the complex plane is due to the proposed controller's ability to effectively dampen the low-frequency modes and improve the system's stability. By moving the roots to the left half side of the complex plane, the critical case, which was previously poorly damped and unstable, becomes stable.

We summarize the results of the eigenvalue analysis of the microgrid system under conventional and modified droop controls. The results show that the modified droop control improves the system's stability by effectively damping the low-frequency modes and shifting the eigenvalues to the left half of the complex plane.

Thus, the proposed controller design can be concluded in the following steps:

- In an inverter-based system, the low-frequency filter introduces a time delay in the system's response to changes in the load.
- The delay can cause the system to respond slowly to changes in the load, leading to undesirable performance.
- To compensate for the delay and improve the system's response time, a lead compensator can be added to the system.
- A lead compensator introduces a phase advance in the system's response, reducing the time delay and improving the response time.
- The concept of the lead compensator is standard in synchronous-based systems but can also be applied to inverter-based systems.
- The compensator's parameters are chosen to meet the desired performance specifications, such as stability, overshoot, settling time, and steady-state error.

4. Simulation Results

A 220 V, 50 Hz, three-phase, three-inverter radial MG system is simulated using MATLAB/Simulink Version 9.12 (R2022a) software. Table 1 shows the system's parameters. All three inverters use the droop control technique with equal droop coefficients to guarantee equal power sharing. Assuming the inverter's input to be a constant DC source, we neglected its dynamics. However, it's worth noting that the DC source may remain relatively constant, as is the case with a battery-powered system. The three inverters are operated in a decentralized manner, demonstrating that no communication between the inverters is required.

Table 1. The test system parameters.

Parameter	Notation	Value
Filter inductance	L_f	1.35 mH
Dc voltage	V_{dc}	700 V
Filter capacitance	C_f	50 μ F
Droop coefficient constraints	m_{p_min}	1×10^{-4}
	m_{p_max}	65×10^{-4}
Coupling inductance	L_l	0.35 mH
Line reactance	X_{ij}	4.71 Ω l
Line resistances	R_{ij}	1.03 Ω l
Voltage controller P gain	K_{pv}	0.168
Voltage controller I gain	K_{iv}	189.34
Current controller P gain	K_{pc}	13.57
Current controller I gain	K_{ic}	1005.3
Feedforward gain	F	0.75
Cutoff frequency of the filter	ω_c	31.4 rad/s
Load power	$P_1, P_2,$	5.8 KW
	P_3, P_4	2.3 KW

The proposed system, illustrated in Figure 1, was subjected to simulation analysis to evaluate its performance with and without the proposed controller. At time $t = 1$ s, a load change occurred, and the system's performance was analyzed and compared in both cases. The simulation results of the system without the proposed controller are presented in Figures 8–11. The droop coefficient used in the simulation is depicted in Figures 8 and 9 and has a value of 5×10^{-4} . Figure 8 shows that the load-sharing and frequency deviation performances are steady. However, due to the slow sharing of power, there would be a frequency mismatch between the inverters for an extended period. This finding highlights the limitations of the conventional droop controller technique in inverter-based IMG systems, which struggles to ensure fast power sharing without compromising system stability. To further analyze the system's performance, Figure 9 displays the system's reactive power and voltage waveforms of the three inverters. This waveform analysis is used to verify the reactive power control operation, which is a critical aspect of the system's performance. The results show that the reactive power control operation is functioning as intended, but the slow power-sharing performance remains a persistent issue. These findings lead to the conclusion that the proposed controller is necessary to improve the performance of the system, particularly in terms of power sharing and frequency deviation. The controller is designed to effectively dampen low-frequency oscillations, even at higher droop gain values, which would typically lead to instability. This approach offers a promising solution to the challenge of achieving fast power sharing and stable performance in inverter-based IMG systems.

After analyzing the simulation results of the system without the proposed controller, this study experimented with increasing the droop value coefficient to improve the power-sharing performance. The droop value coefficient was increased to 20×10^{-4} , as shown in Figure 10. The results show that increasing the droop value coefficient led to a significant improvement in power-sharing performance. However, this improvement came at a cost, as the system's stability became critically compromised. This instability can be attributed to the high droop gain values used to achieve fast power sharing, which can lead to low-frequency oscillations and instability in the system.

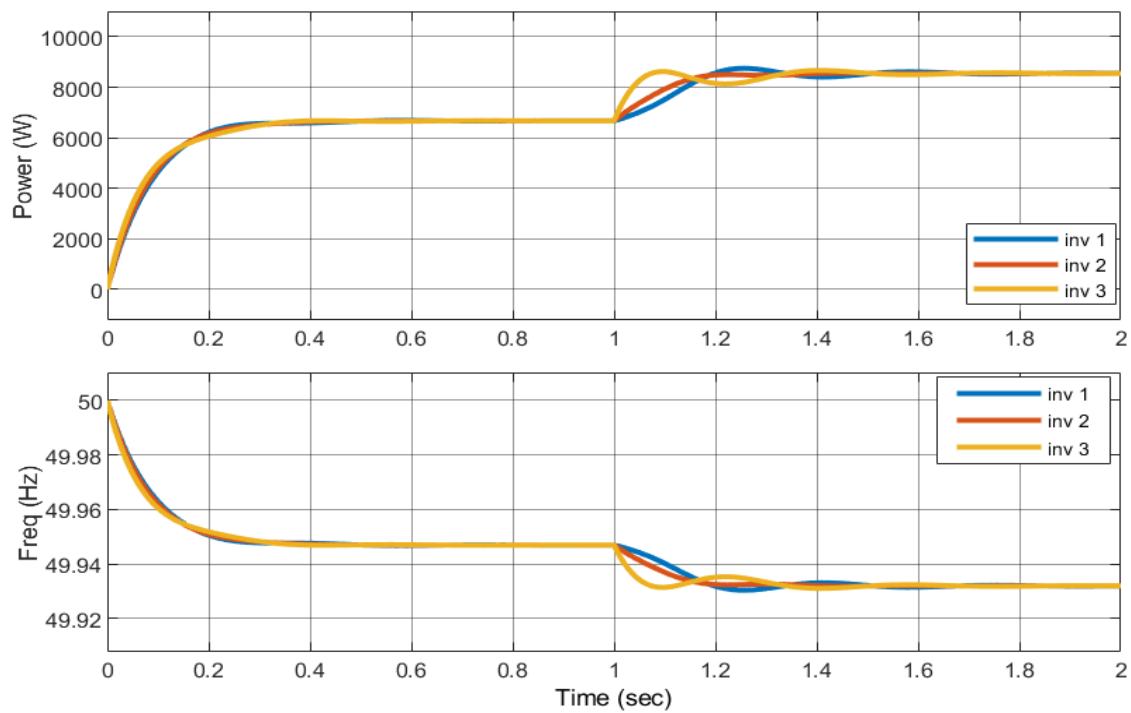


Figure 8. Performance of the conventional controller with $m_p = 5 \times 10^{-4}$.

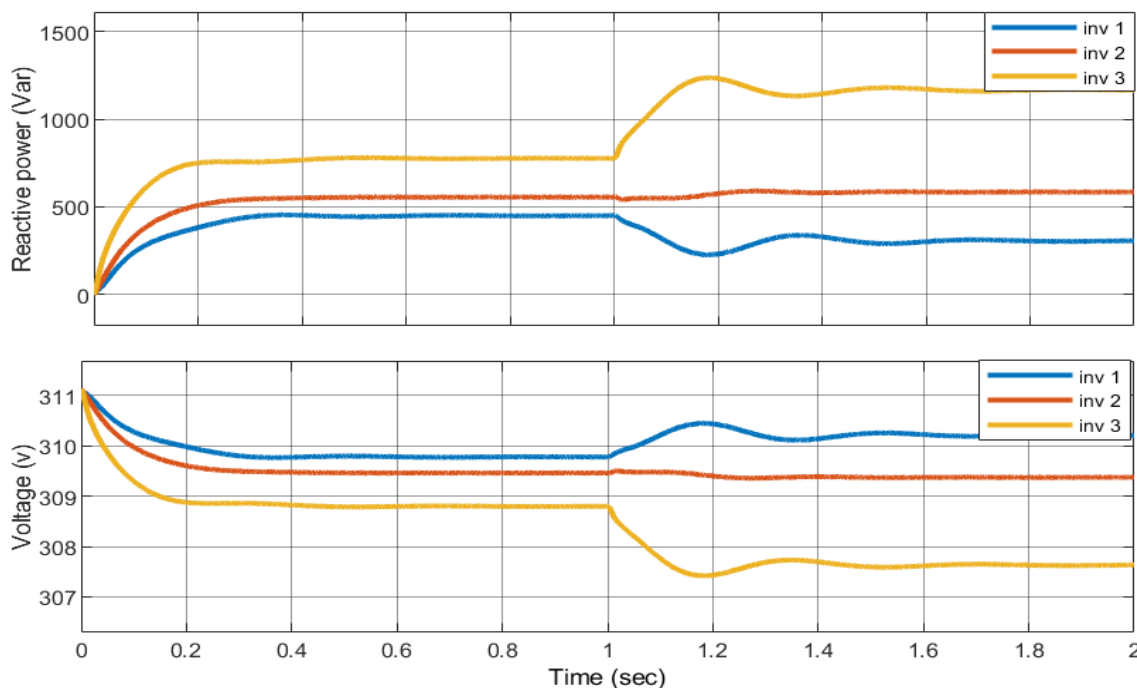


Figure 9. Performance of the conventional controller with $m_p = 5 \times 10^{-4}$ (reactive power and voltage).

Continuing the testing with different droop coefficient values, the researchers increased the droop coefficient to 30×10^{-4} , as shown in Figure 11. The results reveal that this increase in the droop coefficient drove the system to become unstable, with high oscillations in the system frequency. This instability can be attributed to the high droop gain values used, which can lead to low-frequency oscillations and instability in the system. These findings highlight the challenge of balancing the system's fast performance and stability. The system's ability to respond to load changes primarily depends on the value of m_p , making it susceptible to instability and oscillations when the droop coefficient is set too

high. Therefore, a tradeoff in the system’s design between its fast performance and stability should be carefully chosen to ensure optimal system performance.

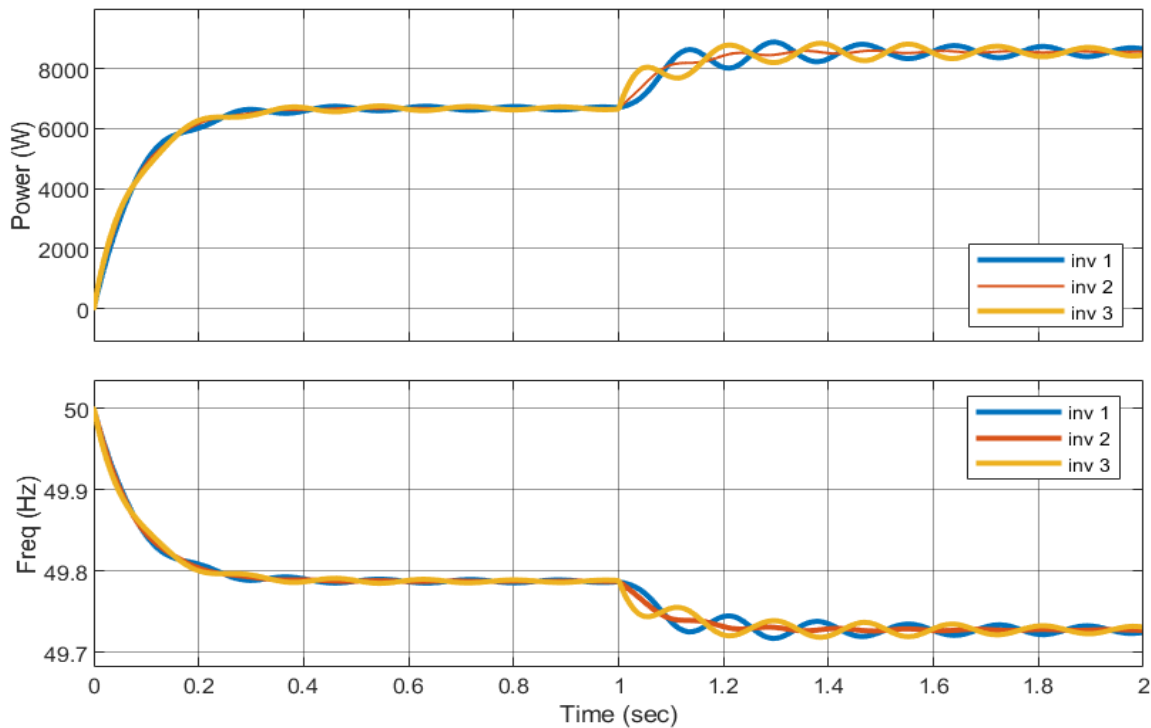


Figure 10. Performance of the conventional controller with $m_p = 20 \times 10^{-4}$.

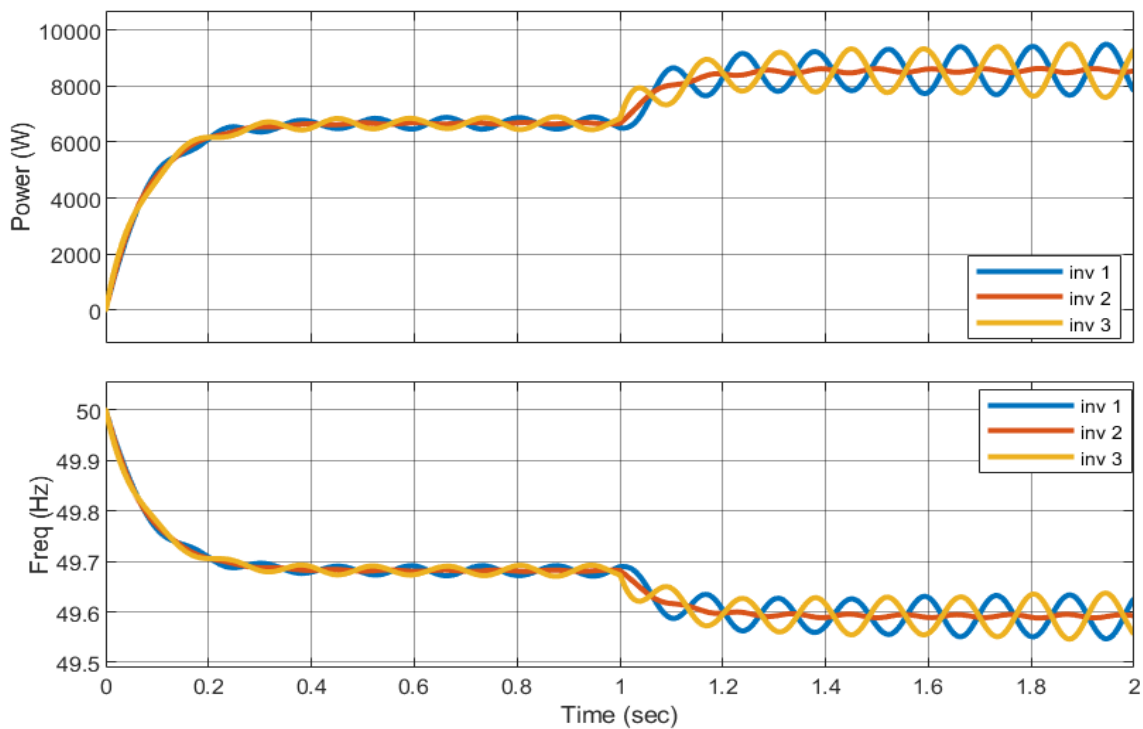


Figure 11. Performance of the conventional controller with $m_p = 30 \times 10^{-4}$.

Figure 12 presents the performance of the microgrid (MG) system for the three inverters under the proposed controller. Due to the scope of this paper, only real power sharing and frequency have been presented. The reactive power and voltage waveforms, although

relevant to the evaluation of the proposed controller, have been omitted due to space constraints and to avoid redundancy. The simulation results show that the proposed controller is effective in improving the performance of the MG system for a range of droop coefficient values, from 5×10^{-4} to 30×10^{-4} (beyond its critical value). The settling time for power sharing and frequency in the system is significantly improved with the introduction of the controller. The results confirm that the proposed controller offers a promising solution to the challenge of achieving fast power sharing and stable performance in inverter-based IMG systems. The proposed controller is designed to effectively dampen low-frequency oscillations, even at higher droop gain values, thereby improving the system's stability without compromising its fast performance. The omission of the reactive power and voltage waveforms from Figure 12 does not diminish their importance in evaluating the proposed controller. Reactive power control is a critical aspect of MG system performance, and the voltage waveform is an essential component of the system's stability.

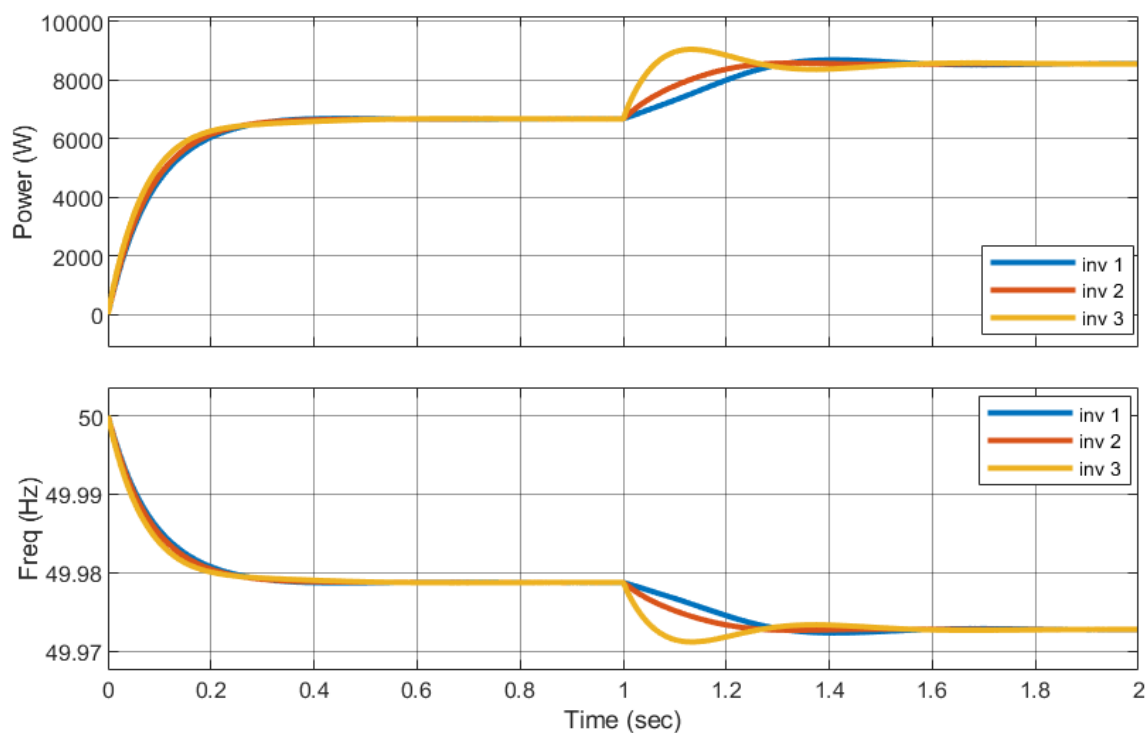


Figure 12. Performance of the proposed controller with $m_p = 5 \times 10^{-4}$.

The stability of the system with $m_p = 30 \times 10^{-4}$ has been verified, highlighting the effectiveness of the proposed controller method in achieving system stability regardless of the droop coefficient value. This finding contrasts with conventional control methods, which rely heavily on the droop coefficient value to achieve stable performance. The results demonstrate that when the proposed controller is applied as an auxiliary signal, power is transferred equitably and correctly between the sources without oscillations, as shown in Figures 13 and 14. This result is achieved even at lower droop coefficients, which means that increasing the droop coefficient is not necessary for precise power sharing. The suggested controller achieves precise power sharing with reduced frequency variations, making it a more robust solution for large droop gain variations compared to conventional techniques. The slight oscillations shown in the simulation results have a minimal effect on the system performance. Therefore, the proposed controller performs better in terms of damping, offering improved performance compared to conventional control methods. In conclusion, the simulation analysis results demonstrate the effectiveness of the proposed controller method in achieving stable and equitable power sharing in inverter-based IMG systems. The proposed controller offers a more robust solution to the challenge of achieving

precise power sharing and system stability, even at lower droop coefficients. The results confirm that the proposed controller outperforms conventional control methods in terms of damping, making it a more effective solution for inverter-based IMG systems.

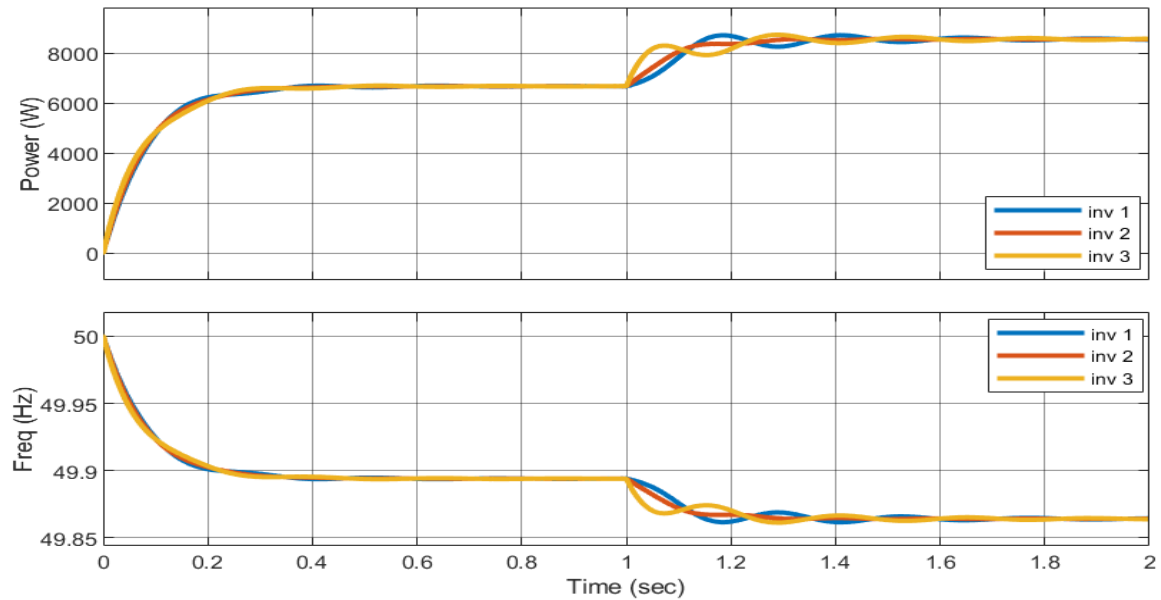


Figure 13. Performance of the proposed controller with $m_p = 20 \times 10^{-4}$.

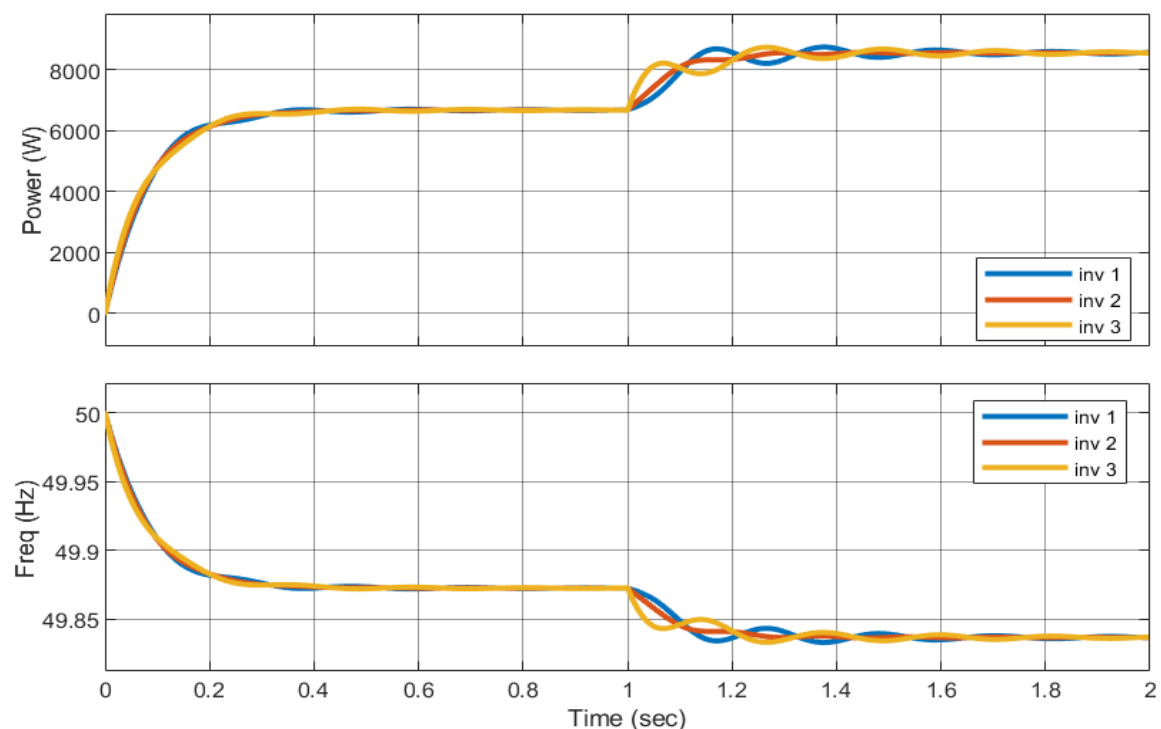


Figure 14. Performance of the proposed controller with $m_p = 30 \times 10^{-4}$.

The simulation results show that the proposed controller outperforms conventional control methods in terms of damping. The slight oscillations shown in the simulation results have a minimal impact on the system's performance, demonstrating the robustness of the controller. The proposed controller offers a more effective solution for inverter-based IMG systems, as it achieves stable and equitable power sharing, even at lower droop coefficients. In summary, the proposed controller addresses the challenges of achieving fast

power sharing and system stability in inverter-based autonomous microgrids. It achieves this by introducing an auxiliary signal that compensates for filter lag, effectively dampening low-frequency oscillations in the system. The stability of the system is verified regardless of the droop coefficient value, making it a more robust solution for large droop gain variations compared to conventional techniques. The simulation results demonstrate that the proposed controller outperforms conventional control methods in terms of damping, making it a more effective solution for inverter-based IMG systems.

Table 2 provides quantitative performance index data analysis, including settling time and overshooting, for both the conventional and proposed controller methods. The results demonstrate that at low droop gain, the proposed controller has a faster settling time compared to the conventional controller. Additionally, when the droop gain is increased to facilitate power sharing, the conventional droop control method fails to reach a steady state or becomes unstable, whereas the proposed technique remains stable and reaches the final steady-state value in less time.

Table 2. Performance index data analysis.

		Conventional Droop Control	Proposed Control
$m_p = 5 \times 10^{-4}$			
Overshooting	Active power	3%	2%
	Frequency	2%	1%
Settling time	Active power	2.2 s	0.7 s
	Frequency	1.5 s	0.54 s
$m_p = 20 \times 10^{-4}$			
Overshooting	Active power	3.2%	1.5%
	Frequency	1.5%	1.2%
Settling time	Active power	1.6 s	0.4 s
	Frequency	1.5 s	0.3 s
$m_p = 30 \times 10^{-4}$			
Overshooting	Active power	4%	2%
	Frequency	3%	1%
Settling time	Active power	NA (unstable)	0.23 s
	Frequency	NA (unstable)	0.11 s

In summary, the quantitative performance index data presented in Table 2 highlight the advantages of the proposed control method over the conventional control method under varying conditions. The data provide valuable insights into the performance of the systems and demonstrate the effectiveness of the proposed technique in achieving stable and efficient power sharing in a multi-inverter system.

In a real application of a droop controller for a microgrid, the choice of control equipment will depend on the specific requirements of the system. If the microgrid is small and relatively simple, a microcontroller may be sufficient to implement the droop controller. Microcontrollers are compact and cost-effective and can be programmed to perform a variety of control tasks. However, for larger and more complex microgrids, an industrial computer may be a better choice. Industrial computers are designed to handle complex tasks such as data acquisition, signal processing, and control, and can be programmed with a variety of software tools. They also offer more processing power and flexibility than a microcontroller, making them more suitable for larger and more complex control applications. Ultimately, the choice of control equipment will depend on the specific needs of the microgrid and the requirements of the droop controller implementation, including factors such as processing power, flexibility, and cost.

Although this paper shows the effectiveness of the proposed controller, some related issues should be studied in future work, such as:

- Investigation of the impact of different types of loads on the performance of the droop controller in an isolated microgrid and development of load-dependent control strategies.
- Development of a hybrid control strategy that combines droop control with other control techniques for improved performance in isolated microgrids.
- Investigation of the impact of renewable energy sources on the performance of the droop controller in an isolated microgrid and development of control strategies that can accommodate fluctuating renewable energy output.

5. Conclusions

This paper proposes a new controller design for an MG-based conventional droop control system. The proposed controller compensates for the lag response caused by the filter delay in the output of the IMG, providing an accurate coefficient for the droop controller—a design problem for conventional droop controllers. The proposed controller design is easy to implement by adding a supplementary signal in parallel with the droop controller loop to dampen the frequency caused by load-sharing between the inverters. The simulation results demonstrate that the suggested controller significantly improves the MG's stability margin at both low and high droop coefficient values while ensuring faster power sharing. The frequency dynamic and steady-state oscillation were reduced, whereas the power-sharing quantities between the inverters remained unaffected. Small signal analysis was also studied to analyze the dynamic performance of the proposed controller. The simulation results under various operating scenarios have been studied to verify the proposed controller, and the results show that the proposed PSS-based droop controller significantly contributes to preserving MG stability and reliability. Overall, the proposed controller-based droop controller offers a more effective solution to the challenge of achieving precise power sharing and system stability in inverter-based IMG systems. The proposed controller improves the system's stability margins, ensures faster power sharing, and reduces oscillations and variations in the system frequency. The proposed controller is easy to implement and demonstrates significant contributions to preserving MG stability and reliability.

Author Contributions: Conceptualization, A.R., T.S. and D.S.M.O.; methodology, A.R., A.M.H., M.E. and D.S.M.O.; software, A.R., A.M. and D.S.M.O.; validation, A.M.H., M.E., A.M. and D.S.M.O.; formal analysis, A.R., A.M. and A.M.H.; investigation, A.R. and D.S.M.O.; resources, A.M., A.M.H. and T.S.; data curation, A.R., D.S.M.O., M.E. and A.M.H.; writing—original draft preparation, A.R. and D.S.M.O.; writing—review and editing, T.S., M.E. and A.M.H.; visualization, A.R. and D.S.M.O.; supervision, T.S. and A.M.H.; project administration, T.S. and A.M.H. All authors have read and agreed to the published version of the manuscript.

Funding: This research received was funded by Russian Science Foundation, No. 23-41-10001 And The APC was funded by A. M.

Informed Consent Statement: Not applicable.

Data Availability Statement: Not applicable.

Acknowledgments: Alexey Mikhaylov's research was funded by a grant from the Russian Science Foundation, No. 23-41-10001, <https://rscf.ru/project/23-41-10001/> (accessed on 12 June 2023).

Conflicts of Interest: The authors declare no conflict of interest.

Abbreviations

MG	Microgrid
DG	Distributed generation
PI	A proportional-integral controller
DC	Direct current
AC	Alternating current
IMG	Isolated microgrid

References

- Hernández-Mayoral, E.; Madrigal-Martínez, M.; Mina-Antonio, J.D.; Iracheta-Cortez, R.; Enríquez-Santiago, J.A.; Rodríguez-Rivera, O.; Martínez-Reyes, G.; Mendoza-Santos, E. A Comprehensive Review on Power-Quality Issues, Optimization Techniques, and Control Strategies of Microgrid Based on Renewable Energy Sources. *Sustainability* **2023**, *15*, 9847. [\[CrossRef\]](#)
- González, I.; Calderón, A.J.; Folgado, F.J. IoT real time system for monitoring lithium-ion battery long-term operation in microgrids. *J. Energy Storage* **2022**, *51*, 104596. [\[CrossRef\]](#)
- Razavi, E.; Arefi, A.; Smith, D.; Ledwich, G.; Nourbakhsh, G.; Minakshi, M. Privacy-Preserved Framework for Short-Term Probabilistic Net Energy Forecasting. *IEEE Trans. Ind. Inform.* **2022**, *19*, 7613–7623. [\[CrossRef\]](#)
- Razavi, S.E.; Arefi, A.; Ledwich, G.; Nourbakhsh, G.; Smith, D.B.; Minakshi, M. From load to net energy forecasting: Short-term residential forecasting for the blend of load and PV behind the meter. *IEEE Access* **2020**, *8*, 224343–224353. [\[CrossRef\]](#)
- Basantes, J.A.; Paredes, D.E.; Llanos, J.R.; Ortiz, D.E.; Burgos, C.D. Energy Management System (EMS) Based on Model Predictive Control (MPC) for an Isolated DC Microgrid. *Energies* **2023**, *16*, 2912. [\[CrossRef\]](#)
- Saad, N.H.; El-Sattar, A.A.; Mansour, A.E.A.M. A novel control strategy for grid connected hybrid renewable energy systems using improved particle swarm optimization. *Ain Shams Eng. J.* **2018**, *9*, 2195–2214. [\[CrossRef\]](#)
- Sarwar, S.; Kirli, D.; Merlin, M.M.C.; Kiprakis, A.E. Major Challenges towards Energy Management and Power Sharing in a Hybrid AC/DC Microgrid: A Review. *Energies* **2022**, *15*, 8851. [\[CrossRef\]](#)
- Tayab, U.B.; Roslan, M.A.B.; Hwai, L.J.; Kashif, M. A review of droop control techniques for microgrid. *Renew. Sustain. Energy Rev.* **2017**, *76*, 717–727. [\[CrossRef\]](#)
- Taher, A.M.; Hasanien, H.M.; Ginidi, A.R.; Taha, A.T. Hierarchical model predictive control for performance enhancement of autonomous microgrids. *Ain Shams Eng. J.* **2021**, *12*, 1867–1881. [\[CrossRef\]](#)
- Abdulmohsen, A.M.; Omran, W.A. Active/reactive power management in islanded microgrids via multi-agent systems. *Int. J. Electr. Power Energy Syst.* **2022**, *135*, 107551. [\[CrossRef\]](#)
- Sun, Y.; Hou, X.; Yang, J.; Han, H.; Su, M.; Guerrero, J.M. New Perspectives on Droop Control in AC Microgrid. *IEEE Trans. Ind. Electron.* **2017**, *64*, 5741–5745. [\[CrossRef\]](#)
- Ferahtia, S.; Djerioui, A.; Rezk, H.; Chouder, A.; Houari, A.; Machmoum, M. Adaptive Droop based Control Strategy for DC Microgrid Including Multiple Batteries Energy Storage Systems. *J. Energy Storage* **2022**, *48*, 103983. [\[CrossRef\]](#)
- Trinh, H.-A.; Truong, H.-V.; Ahn, K.K. Development of Fuzzy-Adaptive Control Based Energy Management Strategy for PEM Fuel Cell Hybrid Tramway System. *Appl. Sci.* **2022**, *12*, 3880. [\[CrossRef\]](#)
- Papageorgiou, P.; Oureilidis, K.; Tsakiri, A.; Christoforidis, G. A Modified Decentralized Droop Control Method to Eliminate Battery Short-Term Operation in a Hybrid Supercapacitor/Battery Energy Storage System. *Energies* **2023**, *16*, 2858. [\[CrossRef\]](#)
- Lu, F.; Liu, H. An Accurate Power Flow Method for Microgrids with Conventional Droop Control. *Energies* **2022**, *15*, 5841. [\[CrossRef\]](#)
- Jasim, A.M.; Jasim, B.H.; Bureš, V.; Mikulecký, P. A New Decentralized Robust Secondary Control for Smart Islanded Microgrids. *Sensors* **2022**, *22*, 8709. [\[CrossRef\]](#)
- Golsorkhi, M.S.; Lu, D.D.C. A Control Method for Inverter-Based Islanded Microgrids Based on V-I Droop Characteristics. *IEEE Trans. Power Deliv.* **2014**, *30*, 1196–1204. [\[CrossRef\]](#)
- Peng, Y.; Shuai, Z.; Liu, X.; Li, Z.; Guerrero, J.M.; Shen, Z.J. Modeling and Stability Analysis of Inverter-Based Microgrid Under Harmonic Conditions. *IEEE Trans. Smart Grid* **2019**, *11*, 1330–1342. [\[CrossRef\]](#)
- Wang, S.; Liu, Z.; Liu, J.; Boroyevich, D.; Burgos, R. Small-Signal Modeling and Stability Prediction of Parallel Droop-Controlled Inverters Based on Terminal Characteristics of Individual Inverters. *IEEE Trans. Power Electron.* **2019**, *35*, 1045–1063. [\[CrossRef\]](#)
- Zhou, B.; Zou, J.; Chung, C.Y.; Wang, H.; Liu, N.; Voropai, N.; Xu, D. Multi-microgrid Energy Management Systems: Architecture, Communication, and Scheduling Strategies. *J. Mod. Power Syst. Clean Energy* **2021**, *9*, 463–476. [\[CrossRef\]](#)
- Al-Sakkaf, S.; Kassas, M.; Khalid, M.; Abido, M.A. An Energy Management System for Residential Autonomous DC Microgrid Using Optimized Fuzzy Logic Controller Considering Economic Dispatch. *Energies* **2019**, *12*, 1457. [\[CrossRef\]](#)
- Bukar, A.L.; Tan, C.W.; Said, D.M.; Dobi, A.M.; Ayop, R.; Alsharif, A. Energy management strategy and capacity planning of an autonomous microgrid: Performance comparison of metaheuristic optimization searching techniques. *Renew. Energy Focus* **2021**, *40*, 48–66. [\[CrossRef\]](#)
- Shabani, H.R.; Kalantar, M. Real-time transient stability detection in the power system with high penetration of DFIG-based wind farms using transient energy function. *Int. J. Electr. Power Energy Syst.* **2021**, *133*, 107319. [\[CrossRef\]](#)

24. Chen, K.; Baran, M. Robust Controller for Community Microgrids for Stability Improvement in Islanded Mode. *IEEE Trans. Power Syst.* **2022**, *38*, 2472–2484. [[CrossRef](#)]
25. Naderi, Y.; Hosseini, S.H.; Zadeh, S.G.; Mohammadi-Ivatloo, B.; Vasquez, J.C.; Guerrero, J. An overview of power quality enhancement techniques applied to distributed generation in electrical distribution networks. *Renew. Sustain. Energy Rev.* **2018**, *93*, 201–214. [[CrossRef](#)]
26. Yanine, F.; Sánchez-Squella, A.; Barrueto, A.; Parejo, A.; Cordova, F.; Rother, H. Grid-Tied Distributed Generation Systems to Sustain the Smart Grid Transformation: Tariff Analysis and Generation Sharing. *Energies* **2020**, *13*, 1187. [[CrossRef](#)]
27. Azizi, A.; Peyghami, S.; Mokhtari, H.; Blaabjerg, F. Autonomous and decentralized load sharing and energy management approach for DC microgrids. *Electr. Power Syst. Res.* **2019**, *177*, 106009. [[CrossRef](#)]
28. Khezri, R.; Golshannavaz, S.; Bevrani, H. Three-Stage Fuzzy Coordinator for Dynamic Stability Enhancement of Multi-Machine Power System Considering Various Penetration Levels of Wind Turbines. *Electr. Power Compon. Syst.* **2018**, *46*, 1185–1197. [[CrossRef](#)]
29. Zhang, L.; Zheng, H.; Hu, Q.; Su, B.; Lyu, L. An Adaptive Droop Control Strategy for Islanded Microgrid Based on Improved Particle Swarm Optimization. *IEEE Access* **2020**, *8*, 3579–3593. [[CrossRef](#)]
30. Firdaus, A.; Mishra, S. Mitigation of Power and Frequency Instability to Improve Load Sharing Among Distributed Inverters in Microgrid Systems. *IEEE Syst. J.* **2019**, *14*, 1024–1033. [[CrossRef](#)]
31. Hassan, M.A.; Worku, M.Y.; Abido, M.A. Optimal Power Control of Inverter-Based Distributed Generations in Grid-Connected Microgrid. *Sustainability* **2019**, *11*, 5828. [[CrossRef](#)]
32. Shan, Y.; Hu, J.; Liu, H. A Holistic Power Management Strategy of Microgrids Based on Model Predictive Control and Particle Swarm Optimization. *IEEE Trans. Ind. Inform.* **2021**, *18*, 5115–5126. [[CrossRef](#)]
33. Aderibole, A.; Zeineldin, H.H.; Al Hosani, M. A critical assessment of oscillatory modes in multi-microgrids comprising of synchronous and inverter-based distributed generation. *IEEE Trans. Smart Grid* **2018**, *10*, 3320–3330. [[CrossRef](#)]
34. Dawoud, N.M.; Megahed, T.F.; Kaddah, S.S. Enhancing the performance of multi-microgrid with high penetration of renewable energy using modified droop control. *Electr. Power Syst. Res.* **2021**, *201*, 107538. [[CrossRef](#)]

Disclaimer/Publisher’s Note: The statements, opinions and data contained in all publications are solely those of the individual author(s) and contributor(s) and not of MDPI and/or the editor(s). MDPI and/or the editor(s) disclaim responsibility for any injury to people or property resulting from any ideas, methods, instructions or products referred to in the content.